

**COMPUTATIONAL DISCOVERY OF NOVEL LOW MICROMOLAR HUMAN PREGNANE X
RECEPTOR ANTAGONISTS**

Sean Ekins, Vladyslav Kholodovych, Ni Ai, Michael Sinz, Joseph Gal, Lajos Gera, William J. Welsh,

Kenneth Bachmann and Sridhar Mani

Collaborations in Chemistry, Jenkintown, PA 19046; Department of Pharmaceutical Sciences, University of Maryland, 20 Penn Street, Baltimore, MD 21201 and Department of Pharmacology, University of Medicine and Dentistry of New Jersey, Robert Wood Johnson Medical School, Piscataway, NJ 08854.

Running title: Novel PXR antagonists

Corresponding authors: Sean Ekins, D.Sc., Collaborations in Chemistry, Jenkintown, PA 19046 Phone 215-687-1320; Fax 215-481-0159; Email ekinssean@yahoo.com

Sridhar Mani, Albert Einstein Cancer Center, Albert Einstein College of Medicine, Bronx, NY 10461, Email smani@montefiore.org

| | |
|------------------------|----------------------|
| Number of Text pages: | 19 |
| Tables: | 3 and 4 supplemental |
| Figures: | 5 and 3 supplemental |
| References: | 50 |
| Words in Abstract: | 250 |
| Words in Introduction: | 952 |
| Words in Discussion: | 2300 |

The abbreviations used are: AF-2, activation function-2; BEI, binding efficiency index; CYP, cytochrome P450; HA, heavy atom count; LBD, ligand binding domain; LE, ligand efficiency; PSA, polar surface area; PXR, pregnane X receptor; QSAR, quantitative structure-activity relationship; SEI, Surface binding efficiency; SMRT, silencing mediator for retinoid and thyroid receptors; SRC-1, steroid receptor coactivator-1;

ABSTRACT

To date there have been very few antagonists identified for the human pregnane X receptor (PXR). These molecules may be of utility for modulating the effects of therapeutic drugs which are potent agonists for this receptor (e.g. some anticancer compounds and macrolide antibiotics), with subsequent effects on transcriptional regulation of xenobiotic metabolism and transporter genes. A recent novel pharmacophore for PXR antagonists was developed using three azoles and consisted of two hydrogen bond acceptor regions and two hydrophobic features. This pharmacophore also suggested an overall small binding site that was identified on the outer surface of the receptor at the AF-2 site and validated by docking studies. Using computational approaches to search libraries of known drugs or commercially available molecules is preferred over random screening. We have now described several new smaller antagonists of PXR discovered with the antagonist pharmacophore with *in vitro* activity in the low micromolar range (SPB03255 (IC₅₀ 6.3 μM) and SPB00574 (IC₅₀ 24.8 μM)). We have also used our computational pharmacophore and docking tools to suggest that most of the known PXR antagonists such as coumestrol and sulforaphane, could also interact on the outer surface of PXR at the AF-2 domain. The involvement of this domain was also suggested by further site-directed mutagenesis work. We have additionally described an FDA approved prodrug, leflunomide (IC₅₀ 6.8 μM) which appears to be a PXR antagonist *in vitro*. These observations are important for predicting whether further molecules may interact with PXR as antagonists *in vivo* with potential therapeutic applications.

INTRODUCTION

Our knowledge of ligand-protein interactions for some of the nuclear hormone receptors is in the nascent stages. This has downstream implications for understanding, predicting and modulating the potential xenobiotic and environmental molecule effects on transcription of key genes in human. For example, the pregnane X receptor, PXR (NR1I2; also known as SXR or PAR) regulates multiple genes including the enzymes CYP3A4 (Bertilsson et al., 1998; Blumberg et al., 1998; Kliewer et al., 1998), CYP2B6 (Goodwin et al., 2001), CYP2C9, as well as the transporter P-glycoprotein (ABCB1) (Synold et al., 2001) and others. There is a very broad structural diversity in the molecules that bind to human PXR from bile salts (Krasowski et al., 2005; Schuetz and Strom, 2001) to anticancer compounds (Ekins et al., 2007; Mani et al., 2005). Several X-ray crystal structures of the ligand binding domain (LBD) of PXR (Watkins et al., 2003a; Watkins et al., 2003b; Watkins et al., 2002; Watkins et al., 2001; Xue et al., 2007b) have determined that it is a large, flexible, mostly hydrophobic site with some key polar residues. PXR also has key interactions with coactivators and corepressors (Johnson et al., 2006; Wang et al., 2006). Binding of the steroid receptor coactivator-1 (SRC-1) to activation function-2 (AF-2) on the surface of PXR is key for stabilizing the receptor (Watkins et al., 2003). In addition, a study using homology modeling and molecular dynamics simulation has been used to assess the interaction of the co-repressor silencing mediator for retinoid and thyroid receptors SMRT with PXR (Wang et al., 2006).

In contrast to other nuclear receptors like the androgen receptor (Bisson et al., 2007; Bohl et al., 2004) and thyroid hormone receptor (Schapira et al., 2003b), the majority of publications on PXR to date have focused primarily on agonists, e.g. those capable of inducing drug metabolism and transporter expression, with clinical implications for drug-drug interactions (Ung et al., 2007). Conversely there have been very few attempts to address antagonism at PXR which could be used to diminish agonist interactions that are unavoidable with some treatments such as with anticancer therapies and macrolide antibiotics like rifampicin (Mani et al., 2005). There have however been previous efforts to generate antagonists at the ligand binding domain (LBD) using a crystal structure of PXR with T-0901317 (Xue et al., 2007a), but this proved to be quite difficult to achieve

(Lemaire et al., 2007). Yet there is a growing list of large and small molecule PXR antagonists which includes ET-743 (IC_{50} 2 nM, molecular weight (MWT) 761.84)(Synold et al., 2001), some polychlorinated biphenyls (K_i 0.6-24.5 μ M) (Tabb et al., 2004), ketoconazole (IC_{50} ~20 μ M, MWT 531.43)(Huang et al., 2007), fluconazole and enilconazole (IC_{50} ~20 μ M, MWT 306.27 and 297.18, respectively)(Wang et al., 2007), sulforaphane (IC_{50} 12 μ M, MWT 177.29)(Zhou et al., 2007), coumestrol (IC_{50} 12 μ M, MWT 268.22)(Wang et al., 2008) and the HIV protease inhibitor A-792611 (IC_{50} ~2 μ M, MWT 804.46)(Healan-Greenberg et al., 2007). The variability in MWT, size and affinity of the antagonists might be indicative of different sites or mechanisms of antagonism. It is also not inconceivable that many of the antagonists are binding the same site by possessing a portion of the required pharmacophore for binding.

We have recently shown the antagonists ketoconazole (Huang et al., 2007), fluconazole and enilconazole (Wang et al., 2007) inhibit the activation of PXR in the presence of paclitaxel, while behaving as weak agonists on their own. Ketoconazole has also been shown to inhibit the PXR-SRC-1 interaction indicative of binding to the AF-2 site and site directed mutagenesis data provided confirmation of the importance of this location (Wang et al., 2007). It was additionally proposed that ketoconazole behaved similar to the histidine residue of SRC-1 in interacting at the AF-2 site (Wang et al., 2007). We have previously tested this hypothesis using computational methods to derive a pharmacophore for the three azole antagonists as well as docking these molecules into regions on the outer surface of PXR (Ekins et al., 2007). This enabled us to define the likely key features and location for where these antagonists bind. The properties of the pharmacophore for this site showed an equal balance between hydrogen bond acceptor and hydrophobic features, differing from the predominantly hydrophobic pharmacophores for agonists. The antagonist binding site was also suggested to overlap with the AF-2 region. Docking ketoconazole into this site showed it occupied two out of three subsites of the motif where SRC-1 interacts. Docking of ketoconazole also indicated that the entire molecule may not be important for interaction with PXR as the piperazine ring was predicted as solvent exposed. In combination with the pharmacophore, it was therefore possible to identify the minimum requirements for a pocket that ketoconazole, fluconazole and enilconazole fitted into, suggesting utility for computer-aided antagonist design (Ekins et al.,

2007). Therefore it is possible that while ET-743 is a very large high affinity antagonist that may interact in the ligand binding pocket of PXR (Synold et al., 2001), azoles, which are generally much smaller, are suggested to interact at the AF-2 site on the PXR surface.

In the current study, we have further validated the previously published PXR antagonist pharmacophore and used it to search databases of molecules for novel PXR antagonists that have undergone *in vitro* testing. We have also used the antagonist pharmacophore to predict whether known published human PXR antagonists are likely to fit into the proposed antagonist pocket. In addition, we have compared results from the pharmacophore and GOLD docking to assess whether either or both of these approaches are useful for PXR antagonist discovery. This represents the first computational modeling using ligand- and protein-based methods to our knowledge that has enabled the prospective discovery of new ‘drug-like’ PXR antagonists verified *in vitro*.

MATERIALS AND METHODS

Materials. The cell culture medium used is DMEM. Lipofectamine 2000, PBS, heat-inactivated fetal bovine serum (FBS), trypsin-EDTA (0.25%), and penicillin-streptomycin were purchased from GIBCO/Invitrogen (Carlsbad, CA). Charcoal/dextran treated fetal bovine serum (FBS) was purchased from Hyclone (Logan, UT). HepG2 cells were obtained from ATCC (Manassas, VA). Human PXR-pcDNA3 and luciferase reporter containing CYP3A4 promoter, CYP3A-Luc, were generated at Bristol-Myers Squibb. White TC-surface 384-well plates were purchased from Perkin Elmer (Boston, MA). Luciferase substrate (Steady-Glo) was purchased from Promega (Madison, WI). Rifampicin, leflunomide and warfarin were purchased from Sigma (St. Louis, MO). Ketoconazole was purchased from BIOMOL International, (Plymouth Meeting, PA, USA), sulforaphane, indomethacin, bestatin, rosmarinic acid and itraconazole were purchased from LKT Laboratories Inc. (St. Paul, MN) and SPB compounds were purchased from Ryan Scientific Inc. (Mt. Pleasant, SC). Individual ketoconazole enantiomers were prepared as described previously (Dilmaghanian et al., 2004).

***In silico* modeling: Catalyst™.** The computational molecular modeling studies were carried out using Catalyst™ in Discovery Studio 1.7 and 2.0 (Accelrys, San Diego, CA) running on either a Centrino or Centrino Duo processor (Intel, Santa Clara, CA). Pharmacophore models attempt to describe the arrangement of key features that are important for biological activity and their generation has been widely described (Clement and Mehl, 2000; Ekins et al., 2007). The previously reported common features PXR antagonist pharmacophore for the equipotent (~10 μM) PXR antagonists enilconazole, ketoconazole and fluconazole (Huang et al., 2007) has been previously described (Ekins et al., 2007). Ketoconazole served as the template molecule to which the other two azoles were aligned using hydrophobic, hydrogen bond acceptor, hydrogen bond donor and ring aromatic features (Ekins et al., 2007). We also generated a van der Waals shape around the enilconazole structure to create a more restrictive shape/feature hypothesis. Molecule databases provided with the Discovery Studio software, such as the MiniMaybridge, a subset of the Maybridge vendor database (2000 molecules) was used for database searching with this pharmacophore. Additional databases listed below were created using structures

in the MDL SDF format prior to conversion to a 3D Catalyst database after generating up to 100 molecule conformations with the FAST conformer generation method within the maximum energy threshold of 20 kcal/mol. The SCUT database (2004) consisted of 579 known drugs in clinical use in the USA selected from the Clinician's Pocket Drug Reference (Gomella and Haist, 2004). This database has previously been used to search for substrates and inhibitors for the transporters P-glycoprotein (Chang et al., 2006a) and human peptide transporter (Ekins et al., 2005). The BIOMOL natural products database contains 481 molecules and BIOMOL known bioactives database contains 473 molecules which were also converted into separate Catalyst databases. For the database mapping we used rigid fitting and restricted the maximum omitted features to zero (the maximum number of pharmacophore features not mapped by the molecule).

For molecules not retrieved from databases, the structures were sketched in ChemDraw for Excel (CambridgeSoft, Cambridge MA) and exported as sdf files. In Catalyst, the 3-D molecular structures were produced using up to 255 conformers with the 'best' conformer generation method, allowing a maximum energy threshold of 20 kcal/mol for each conformer. Using the Ligand Pharmacophore Mapping protocol the 'Best Mapping' was performed with the 'rigid fitting method' and maximum omitted features set to zero. However for the coumestrols and sulforaphane, the maximum omitted features were increased to 2 as these were found to miss one or more feature. The quality of the molecule mapping to the pharmacophore is determined by the fit value, with a higher fit value representative of a better fit and dependent on the proximity of the features to pharmacophore centroids and the weights assigned to each feature.

Substructure searching. The molecule SPB 03255 was used as a query for substructure searching using two databases that contain information on commercially available molecules namely, ChemSpider (<http://www.chemspider.com/>) and eMolecules (<http://emolecules.com/databases>). The 2D molecular structures of retrieved molecules of interest were converted to 3D conformations in Catalyst (as described above) and fitted with the PXR antagonist pharmacophore as well as the PXR pharmacophore with the enilconazole shape/feature restriction.

***In silico* modeling: docking antagonists to the crystal structure using GOLD.** Protein preparation for GOLD docking (Jones et al., 1997) was done in Sybyl 7.2 (Tripos Inc, St.Louis, MO). The larger fragment of chain A, Ser192-Gly433 from the Protein Databank entry 1NRL was chosen for protein site preparation. Water molecules, salt ions, ligands and co-receptor fragments were deleted. After addition of hydrogen atoms and assigning of the AMBER 02 forcefield charges to the protein, only hydrogen position energy optimization was performed. The resulting protein was saved in Tripos mol2 format and used later as a docking site in GOLD.

The 1NRL chain A was used for rigid docking in which the protein was fixed and only flexibility was allowed for ligands. Each ligand was set to dock 20 times. The previously described (Ekins et al., 2007). docking site (AF-2 site) was defined around the atom on the protruding tip of SRC-1. x 3.582, y 16.389, z 21.454 with a radius of 5 Å.

Cell Culture, PXR Transactivation and Cytotoxicity Assays. The assays used to determine PXR agonists and antagonists have been previously described in detail and the reader is also referred to these (Huang et al., 2007; Mani et al., 2005; Wang et al., 2007; Wang et al., 2008). Culture of HepG2 cells was performed in T175 flasks using DMEM containing 10% FBS. The transfection mixture contains 1 µg/ml of PXR-pcDNA3 plasmid DNA, 20 µg/ml of Cyp3A-Luc plasmid DNA, 90 µl/ml of Lipofectamine 2000, and serum-free medium. After incubating at room temperature for 20 min, the transfection mixture (1 ml per flask) was applied to the cells in fresh medium (20 ml per flask), and flasks incubated at 37°C (5% CO₂) overnight. Following the transient transfection, cells were trypsinized and cryopreserved for long-term storage.

On the day of the experiment, vials of cryopreserved cells were thawed and then re-suspended in fresh (DMEM containing 5% charcoal/dextran-treated FBS, 1% penicillin/streptomycin, 100 µM non-essential amino acids, 1 mM sodium pyruvate, and 2 mM L-glutamine). 50µl microliters of cell mixture (8 x 10³ cells) was added to wells of white tissue-culture treated 384-well plates containing either 0.5 µl of test compound alone or a mixture of test compound and rifampicin (10 µM) dissolved in 100% DMSO.

The plates were incubated at 37°C (5% CO₂) for 24 hr, then 5 µl of Alamar Blue reagent (Trek Diagnostics, Cat #00-100) was added to each well. Plates were then incubated for an additional 2 hr at 37 °C, 5% CO₂ and then 1 hr at room temperature. Fluorescence was read at ex525/em598 (nm). After the fluorescence is measured, 25 µl of luciferase substrate (Steady-Glo, Promega) was added to each well. The plates were incubated for 15 min at room temperature, after which the luminescence was read on a Viewlux (Perkin-Elmer) plate reader. In addition, drug induced cytotoxicity was assessed by the MTT assay in cancer cell lines (LS174T and SKOV3) as well as fibroblast cells (CRL) (Ekins et al., 2007; Estebanez-Perpina et al., 2007). Cells were exposed to a concentration range of the drug(s) for 48 hr. These assays were repeated three separate times, each in triplicate.

Site Directed Mutagenesis. A site-specific mutation was made using Quick-Change-II Site-Directed Mutagenesis Kit (Stratagene, La Jolla, CA) protocol for PCR using manufacturer guidelines. The following primers were used (underlines indicate mutated nucleotides)

Q272H(Forward): 5'-ttgccatcgaggacCATtatctccctgctg-3'

Q272H(Reverse): 5'-cagcagggagatATGgtcctcgatgggcaa-3'

The mutation was generated using pSG5-PXR plasmid (Steve Kliewer, UT Southwestern) as a template. XL-blue competent cells were used to transform the PCR product(s) and bacterial colonies were used to isolate plasmid DNA. The clone was sequenced to confirm and verify the mutation.

Transfection Assay. CV-1 and 293T cells were transfected with PXR and reporter plasmids as indicated and previously published (Wang et al., 2008).

Data Analysis. Rifampicin (10 µM), a well known agonist of PXR, is included in each plate as an internal standard and positive control. The data is then expressed as percent activation (% Act), where the total signal is the signal from the 10 µM rifampicin and the blank signal is that from the DMSO vehicle.

$$\% \text{Act} = \frac{\text{Compound signal} - \text{Blank signal}}{\text{Total signal} - \text{Blank signal}} \times 100\%$$

Compounds are tested at ten concentrations (50 μM – 2.5 nM, 1:3 serial dilution). For PXR activation, a plot of concentration vs. % Act was generated for each compound tested. For the plot, concentrations of compound at which 50% activation occurs (EC_{50}) are reported. For PXR inhibition where the cells are incubated with 10 μM rifampicin and a concentration of test compound, % inhibition (%Inh) was calculated (%Inh = 100 - %Act). Concentrations of compound at which 50% inhibition occurs (IC_{50}) are reported and is the mean of duplicate measurements unless otherwise stated.

RESULTS

Fitting known PXR antagonists to the pharmacophore. Enilconazole was mapped to the previously reported pharmacophore for PXR antagonists (Ekins et al., 2007) and the van der Waals shape of the molecule was used to produce a shape/feature pharmacophore (Figure 1A). An interesting observation while creating this hypothesis was that enilconazole does not appear to map to the central hydrogen bond acceptor so it is possible this is not a key interaction for all antagonists and rather represents a common feature in fluconazole and ketoconazole, the other two molecules used to derive the HIPHOP pharmacophore. Sulfuraphane, coumestrol and their analogs were fitted to the PXR antagonist pharmacophore (Figure 1), in the case of the coumestrols (Figure 1B-D) these failed to map at least one feature whereas sulfuraphane missed two features (Figure 1E) and the two isomers scored similarly (Table 1). Previously reported biphenyl PXR antagonists (Tabb et al., 2004) analyzed, map to the hydrophobic features only, missing the hydrogen bond acceptors (Figure 1F). The HIV protease inhibitor A-792611, recently identified as a PXR antagonist (Healan-Greenberg et al., 2007) fitted to all the pharmacophore features once the shape restriction was removed, however there was a substantial amount of the molecule outside of the pharmacophore which might be indicative of potential for unfavorable steric clashes with the protein or solvent exposure (Supplemental Figure 1).

Azole PXR antagonist pharmacophore database searching. The PXR antagonist pharmacophore was used to search the SCUT database of approximately 600 widely prescribed drugs in order to identify non-azole drug molecules as potential antagonists. This pharmacophore was initially found to be quite non-selective as several hundred hits were retrieved. One approach to improve the selectivity of the pharmacophore was to add the van der Waals surface to enilconazole, one of the smaller azoles, when mapped to the pharmacophore (as described above), creating a shape/feature hypothesis (Figure 1A). This shape/feature hypothesis was then used to search the SCUT database and was found to be more restrictive, returning just 11 molecules (Supplemental Table 1) including four azoles (econazole, tioconazole, voriconazole and fluconazole). The latter was used in the initial pharmacophore model development. Indomethacin and warfarin were selected from this list based on their mapping to the pharmacophore and predicted fit (Table 1, Figure 2A) and were tested *in vitro*. The

'BIOMOL natural products' database retrieved two hits (Supplemental Table 2) and one of these, Rosmarinic acid (Table 1, Figure 2B) was tested *in vitro*. Searching the 'BIOMOL known bioactives' database retrieved five hits (Supplemental Table 3), and bestatin (Table 1, Figure 2C) was selected for testing. Forty nine hits were retrieved from the MiniMaybridge database (Supplemental Table 4) and three of the highest scoring hits including SPB03064 (Figure 2D), SPB00574 (Figure 2E) and SPB03255 (Figure 2F) were selected for testing *in vitro*. In all cases these molecules selected for testing appear to fit well to the pharmacophore.

Substructure searching. Based on the greater than 90% structural similarity using the Tanimoto coefficient (ChemFinder, CambridgeSoft, Cambridge, MA) between fluconazole and itraconazole (Ekins et al., 2007) this latter molecule was also selected for *in vitro* testing. In addition, the molecule SPB03255 was used as a query for substructure searching using the internet chemistry databases ChemSpider and eMolecules and suggested 18 structurally similar molecules (Table 2, Figure 3, Supplemental Figure 2) which were fitted to the PXR antagonist pharmacophore as well as the pharmacophore with shape. Several of the smaller molecules do not fit as well to the pharmacophore (no fit values) and these molecules were selected to delineate which part of the molecule are most important for antagonist activity. Leflunomide, which is similar in structure to SPB03255, is an FDA approved antirheumatic drug (Rozman, 2002) that was selected for testing based on its commercial availability.

Docking of antagonists. Several of the known PXR antagonists were docked using GOLD and are shown in Figure 3 including ketoconazole (GOLD score 50.98, Table 1 (Ekins et al., 2007), Figure 4A), coumestrol (GOLD score 33.35, Figure 4B) as well as newly discovered antagonists SPB03255 (GOLD score 38.22, Figure 4C) and SPB06257 (GOLD score 47.26, Figure 4D). Coumestrol, a flat structure lays across the AF-2 site, while SPB03255 fills a part of the pocket in the same manner as the azoles and SPB06257 extends out of the AF-2 pocket onto the surface. The sulforaphane isomers scored similarly (GOLD score 30, Table 1) while A-792611 had a slightly better fit (GOLD score 34.82). Interestingly, itraconazole scored similarly to ketoconazole (GOLD score 51.44, Table 1) and while there was no apparent direct correlation between antagonist activity and GOLD score, we did find that in general those scored the highest were likely to be more

active *in vitro*. For example, of the four molecules tested with the highest GOLD score, three of them were found to be antagonists (Table 2). However, it should be noted that leflunomide was one of the lowest scoring molecules (Table 2) and yet it had comparable activity to SPB03255 which scored higher (Table 1).

***In vitro* data.** Ketoconazole was used as a positive control as an example of a known antagonist and has the approximately the same effect inhibiting the activation of rifampicin as in previous studies with paclitaxel (Table 1) (Huang et al., 2007; Wang et al., 2007). We have also tested the (+) -2R, 4S and (-) -2S, 4R enantiomers of ketoconazole and these appear to show no significant difference in their antagonistic effect (Table 1). Itraconazole was slightly more potent than ketoconazole (IC₅₀ 8.96 μM). The previously shown antagonist sulforaphane was also tested as separate isomers and both were found to be more active (IC₅₀ 5.6 μM) than the previously published racemate and the antagonist coumestrol, both with reported IC₅₀'s of 12 μM (Wang et al., 2008; Zhou et al., 2007). Rifampicin was used as a known PXR agonist and the EC₅₀ reported here is similar to those in other studies in HepG2 and other cell lines (EC₅₀ 400 nM (Hurst and Waxman, 2004)), such as, CV-1 (EC₅₀ 700-852 nM (Chrencik et al., 2005)) and (EC₅₀ 710 nM (Moore et al., 2000)).

From the initial PXR antagonist pharmacophore searching, several molecules were tested *in vitro*. Indomethacin, rosmarinic acid, warfarin, bestatin and SPB 03064 were inactive (Table 1), while SPB00574 was active (IC₅₀ 24.8 μM) and SPB03255 was more active (IC₅₀ 6.3 μM). None of these compounds were found to be significant PXR agonists *in vitro*. Additional PXR antagonist analogs of SPB03255 were identified including SPB03256, SPB06061, SPB06257 and SPB02372. However, SPB03213, SPB03254, SPB03211 and SPB03663 were found to be selective agonists (Table 2 and Supplemental Figure 2).

Site Directed Mutagenesis. Based on previous modeling predictions of the AF-2 contact residues with ketoconazole, the glutamine residue 272 was mutated to histidine (Q272H). The reasons for creating such a PXR mutant came from an ongoing yeast two-hybrid study in which several random mutants of PXR were generated and tested as a bait library using SRC-1 as prey. In this system, we picked several (> 10) colonies of yeast that appeared to be immune from the inhibitory effects of ketoconazole. In all these colonies, there was a Q272H mutation which was present either alone or in combination with other LBD and non-LBD mutants

(unpublished results). We decided to test the single Q272H mutant in a mammalian system to see if this mutant was (1) able to activate upon ligand (agonist) binding; (2) constitutively active and/or (3) immune to the inhibitory effects of ketoconazole. Furthermore, an analog of ketoconazole (compound 3) (Das et al., 2008) lacking the imidazole group but with a 2,4-difluoro substitution of the chloride atoms, resulted in a compound likely lacking contact with Q272. PXR transcription studies in CV-1 cells were performed using the Q272H mutant of PXR cloned into a mammalian plasmid. The wild-type PXR plasmid was activated by rifampicin (2.3-fold) and was significantly inhibited by ketoconazole ($p < 0.0001$). The Q272H mutant of PXR was constitutively active and rifampicin did not significantly augment basal activity. However, this mutant was not inhibited by ketoconazole (Figure 5; $p=0.181$). In contrast, compound 3 inhibited the Q272H mutant in the absence or presence of rifampicin ($p < 0.001$; $p < 0.003$).

DISCUSSION

PXR antagonist pharmacophore database searching. We have previously described the first PXR antagonist pharmacophore which represents a region of the AF-2 domain on the outer surface of the protein and conforms to the site directed mutagenesis and other *in vitro* data (Ekins et al., 2007). Although ketoconazole, enilconazole and fluconazole were reported to be equipotent antagonists of PXR (Huang et al., 2007; Wang et al., 2007) we have also suggested that the entire ketoconazole structure may be unnecessary for antagonist activity. These three azole antagonists are proposed to partially mimic, displace or interfere with the co-activator SRC-1 binding at the AF-two site or close to this region, suggesting a therapeutic option for control of PXR-mediated transcription of target genes in cancer or to counter drug-drug interactions. The PXR antagonist pharmacophore also suggests a relatively small pocket with a balance of hydrogen bond acceptor and hydrophobic interactions (Ekins et al., 2007). We have indicated that computational methods could be useful to further explore the antagonist binding site by database searching in a higher throughput fashion than feasible by random screening *in vitro*. The approaches taken in this study include use of the antagonist pharmacophore and docking molecules into the proposed antagonist site followed by *in vitro* verification. Precedent for such an approach using pharmacophores alone already exists to define new transporter inhibitors and substrates (Chang et al., 2006b; Ekins et al., 2005), although to our knowledge this is the first application of both ligand-based and structure-based (docking) methods to find PXR antagonists. Our hypothesis was that smaller molecules could be at least as active as ketoconazole.

In the current study we first fitted several diverse known PXR antagonists (Tabb et al., 2004; Wang et al., 2007; Zhou et al., 2007) to the pharmacophore to indicate coumestrol, sulforaphane and A-792611 could potentially fit in the AF-2 site, based on the pharmacophore feature mapping (Figure 1, Supplemental Figure 1). The recently identified phytoestrogen coumestrol (Wang et al., 2008) possesses 2 hydroxyl groups as well as several other oxygen atoms that could serve as hydrogen bond acceptors. When the enilconazole van der Waals shape (Figure 1A) is absent from the pharmacophore, the coumestrol molecule fits three features, both hydrogen bond acceptors and the ring aromatic feature, while omitting a hydrophobic feature (Figure 1B). This suggests

coumestrol may bind the same site as the azoles, though the fit is perhaps suboptimal. Docking (Figure 3) also indicates that coumestrol (Figure 3C) may not fit ideally in this site. The two inactive analogs of coumestrol, the diacetate (Figure 1C, D) and coumestrol dimethyl ether fit to the features (Figure 1D) however they extend beyond the enilconazole shape. In the case of the coumestrol dimethyl ether, the molecule is positioned 90 degrees perpendicular to the original coumestrol mapping. Sulforaphane is a naturally occurring PXR antagonist (Zhou et al., 2007) that was found to only fit to the hydrogen bond acceptor features of the PXR antagonist pharmacophore (Figure 1E). This provided weaker evidence that it could bind to the same external PXR surface site as the azoles, so it is possible that some pharmacophore features are more important than others. Similarly we have found that an array of polychlorinated biphenyls (Tabb et al., 2004) may only map to the hydrophobic features of the pharmacophore (Figure 1F). A-792611 could fit to all the pharmacophore features when the enilconazole shape was removed from the pharmacophore, which also suggests that a large percentage of the molecule could be outside of these pharmacophore features (Supplemental Figure 1) much like the case with ketoconazole. The published experimental *in vitro* studies left open the possibility that A-792611 could bind outside of the PXR LBD (Healan-Greenberg et al., 2007). From our pharmacophore analysis it is a distinct possibility that all of the published PXR antagonists could be interacting at the AF-2 site like the azoles.

We have also used the PXR antagonist pharmacophore to search molecule databases in order to discover novel antagonists. After our rather focused screening four databases, representing 3533 molecules, 67 hits were computationally retrieved (Supplemental Tables). We tested *in vitro* a selection of these molecules based on their pharmacophore fit values and visual mapping to the pharmacophore features (Table 1), of which 2 initial molecules represented novel non-azole antagonists, namely SPB03255 (IC₅₀ 6.3 μM) and SPB00574 (IC₅₀ 24.8 μM, Figure 2). SPB03255 and SPB00574 also scored highly based on the pharmacophore fit (Table 1). One high scoring compound inactive *in vitro* (a false positive), SPB03064, contains an N-N bond which is possibly unstable during the incubation period *in vitro*. Indomethacin, bestatin, warfarin, rosmarinic acid were also false positives and represent larger molecules that are lower scoring in terms of fit to the pharmacophore features and may not fit in the antagonist site as well. These inactive molecules may be useful to refine the pharmacophore in

future. It is also interesting to note that the antagonist SPB00574 (Figure 2E) is similar in structure to C2BA-6 (differing in a chlorine substituted ring at the hydroxyl and other chlorine substitutions elsewhere) which was previously reported as a PXR agonist (EC_{50} 1.89 μ M) (Lemaire et al., 2007). In our study, SPB00574 did not appear to show appreciable PXR agonist activity.

One of the novel antagonists SPB03255, was used as a foundation for substructure searching of 2 very large databases to generate a structure activity relationship around this lead molecule. The chemistry databases ChemSpider and eMolecules contained approximately 20 million and 7 million molecules, respectively at the time of use, and enabled us to retrieve 18 structurally similar molecules to SPB03255. These molecules (Table 2, Supplementary Figure 2) were also scored with the PXR antagonist pharmacophore suggesting that several of the molecules had Catalyst fit scores similar or higher than the original molecule. We also discovered that SPB03213, SPB03254, SPB03211 and SPB03663 were selective PXR agonists *in vitro* (Table 2 and Supplemental Figure 2). Three of these had a distinctly different substitution of the phenyl ring with chlorine, compared to the antagonist molecules with chlorine substitutions (Figure 3). This is reminiscent of biphenyl compounds, some of which were antagonists, where it was hypothesized that the arrangement of the chlorines in a square or triangle pattern was a predictor of antagonism (Tabb et al., 2004). In this current study, hydrophobicity on the phenyl ring of the SPB compounds is mainly achieved with methyl or trifluoromethyl groups and the positioning is important. These relatively small PXR antagonists may of course flip inside the AF-2 site and so it is quite difficult to definitively locate potential ligand-protein interactions. It is also of interest that the anti-rheumatic compound leflunomide (IC_{50} 6.8 μ M) possesses a similar substructure to these active SPB compounds, although it possesses an amide linker. Leflunomide has also previously been reported to undergo N-O bond cleavage to the α -cyanoenol metabolite A771726 (Kalgutkar et al., 2003). which achieves median steady-state unbound plasma concentrations of approximately 1.1 μ M.(Chan et al., 2005). Interestingly, both leflunomide and A771726 mapped to the PXR antagonist pharmacophore with fit scores of 2.76 and 1.87, respectively, suggesting both leflunomide and A771726 could behave as PXR antagonists (Supplemental Figure 3). Future work will evaluate whether we are observing the PXR antagonist effect via the metabolite.

Docking of molecules into the AF-2 antagonist site. We used a validated method for docking molecules into the AF-2 site namely, GOLD (Evers et al., 2005; Evers and Klabunde, 2005; Jones et al., 1997) and found that several molecules tested initially (Table 1) scored from 35-45 (lower than ketoconazole (51)) and did not correlate with the *in vitro* activity. Itraconazole scored similarly to ketoconazole and was more active *in vitro*. We also tested 2 ketoconazole enantiomers (2R, 4S and 2S, 4R) and found them to have identical docking scores and *in vitro* activity. Previously modest enantioselective differences were shown for the same two ketoconazole enantiomers as inhibitors of CYP3A4 mediated testosterone and methadone metabolism (Dilmaghanian et al., 2004). In contrast, we found the docking scores of the 2R, 4R enantiomer had a higher docking score of 56.45 and the 2S, 4S enantiomer had a lower docking score of 49.24. To date we have not tested these latter two enantiomers *in vitro*. S- and R- Sulforaphane isomers were also similarly active with almost identical docking scores. Other known antagonists, coumestrol and A-792611, had docking scores from 30-34.8, which are low (Table 1), although visualizing coumestrol suggested it could fit in the AF-2 site. Our docking scores for the compounds that were selected for testing were generally higher in the most active molecules, in the 40-47 range. Docking may therefore be a useful addition to pharmacophores for filtering molecules for optimization.

Several groups have developed relatively simple approaches for guiding molecule optimization in drug discovery based on “ligand efficiency” which normalizes the binding affinity at the target with properties such as molecular weight, number of heavy atoms or polar surface area (Abad-Zapatero and Metz, 2005; Hopkins et al., 2004; Reynolds et al., 2008). When we consider the PXR antagonists from Tables 1 and 2 compared to ketoconazole, the smallest molecules such as sulforaphane and leflunomide have the highest efficiency when measured by any of the three indices (Table 3). Coumestrol has similar efficiency for binding but not for the surface-binding index, due to its high polar surface area. Leflunomide and all of the SPB molecules have approximately 2-fold higher ligand and surface-binding efficiencies than ketoconazole, which is perhaps not surprising given their smaller size. When we consider the ligand efficiency versus heavy atom count (no hydrogens) in Table 3 there is an exponential decrease in efficiency between 10-20 heavy atoms (data not

shown), which is in line with observations of others for much larger datasets across different targets (Reynolds et al., 2008). Such calculated indices may therefore be useful when assessing and comparing future molecules as PXR antagonists.

Site Directed Mutagenesis. Previous site directed mutagenesis studies had suggested that ketoconazole was binding on the outer surface of PXR (Wang et al., 2007). The Q272H mutation undertaken in this study is in the AF-2 cleft and is conservative (glutamine to histidine). These two amino acids are isostructural with regards to polar atoms on glutamine. Based on crystal structure data (Watkins et al., 2003; Xue et al., 2007b) with the SRC-1 peptide, isostructural changes are likely not to disrupt coactivator binding and thus, these mutants are active, especially upon ligand (agonist) binding. However, in our previous paper (Ekins et al., 2007), we predicted that Q272 is an important contact residue for the imidazole ring of ketoconazole in one binding orientation. Our data shows that in fact, substitution with the bulky histidine ring can block ketoconazole binding to PXR while a ketoconazole analog compound 3 (Figure 5, synthesis to be described elsewhere (Das et al., 2008)) that lacks the imidazole ring and substitutes the chlorines with fluorines, retains antagonism of the Q272H mutant (Das et al., 2008). These data validate a residue interaction prediction based on our previously published computational data (Ekins et al., 2007) and provides further confidence that these antagonists are likely to bind in the AF-2 site.

We have utilized the previously published human PXR antagonist pharmacophore to discover new PXR antagonists that were verified *in vitro*. In addition we have used docking, an approach that has been widely applied elsewhere for virtual discovery of new leads for nuclear hormone receptors (Schapira et al., 2003a; Schapira et al., 2003b; Schapira et al., 2000; Schapira et al., 2001) as well as many other therapeutic targets (Bisson et al., 2007; Leach et al., 2006; Zhang et al., 2007). We found that although some of the antagonists such as ketoconazole and itraconazole generally score well this may be because the docking program picks up non-specific van der Waals interactions of large molecules on the outer surface of the AF-2 site. The smaller antagonists discovered such as SPB03255 generally do not have very high docking scores. It would appear that

using the PXR pharmacophore may therefore be a useful tool for rapid screening of molecule databases and identifying potential antagonists that can be followed up with docking. These molecules in turn will need further preclinical assessment to ensure that they are likely to progress as potential clinical candidates (Ekins et al., 2007; Huang et al., 2007; Wang et al., 2007). Potential important applications of PXR antagonists include prevention of drug-drug interactions and potential changes in drug pharmacokinetics. We and others have shown PXR activation can lead to cancer cell proliferation and drug resistance, therefore blocking drug induced PXR activation can mitigate antiapoptotic effects of certain xenobiotics (Chen et al., 2007; Gupta et al., 2008). PXR also induces P-glycoprotein at the blood brain barrier increasing drug efflux from the brain and tightens this barrier (Bauer et al., 2004; Bauer et al., 2006). Interference with this could increase retention of drugs in the CNS when desired.

In summary, we have described several new smaller more efficient antagonists of PXR, to follow on from the initial azoles (such as ketoconazole) identified previously. These molecules have *in vitro* activity in the low micromolar range which is similar to the sulforaphane isomers, and itraconazole. We have also used our computational pharmacophore and docking tools to suggest that most of the known PXR antagonists could also interact on the outer surface of PXR at the AF-2 domain, which is also supported by further site-directed mutagenesis work undertaken in this study with a ketoconazole analog that is lacking the imidazole group. We have also described for the first time that an FDA approved prodrug leflunomide, appears to be a PXR antagonist *in vitro*. Further studies will be important to describe the clinical relevance of this and other antagonists identified to date, to suggest other analogs that may have applications in modulating PXR activity and downstream gene expression *in vivo* for cancer, pharmacokinetics or drug resistance applications.

ACKNOWLEDGMENTS

S.E. gratefully acknowledges Dr. Maggie A.Z. Hupcey for her support, Dr. Matthew D. Krasowski (University of Pittsburgh) for providing the BIOMOL sdf files, Dr. Sean Kim for support of the PXR transactivation assay,

Accelrys, San Diego, CA for making Discovery Studio Catalyst available and the reviewers for their useful suggestions.

REFERENCES

- Abad-Zapatero C and Metz JT (2005) Ligand efficiency indices as guideposts for drug discovery. *Drug Disc Today* **10**(7):464-469.
- Bauer B, Hartz AM, Fricker G and Miller DS (2004) Pregnane X receptor up-regulation of P-glycoprotein expression and transport function at the blood-brain barrier. *Mol Pharm* **66**(3):413-419.
- Bauer B, Yang X, Hartz AM, Olson ER, Zhao R, Kalvass JC, Pollack GM and Miller DS (2006) In vivo activation of human pregnane X receptor tightens the blood-brain barrier to methadone through P-glycoprotein up-regulation. *Mol Pharm* **70**(4):1212-1219.
- Bertilsson G, Heidrich J, Svensson K, Asman M, Jendeberg L, Sydow-Backman M, Ohlsson R, Postlind H, Blomquist P and Berkenstam A (1998) Identification of a human nuclear receptor defines a new signaling pathway for CYP3A induction. *Proc Natl Acad Sci USA* **95**(21):12208-12213.
- Bisson WH, Cheltsov AV, Bruey-Sedano N, Lin B, Chen J, Goldberger N, May LT, Christopoulos A, Dalton JT, Sexton PM, Zhang XK and Abagyan R (2007) Discovery of antiandrogen activity of nonsteroidal scaffolds of marketed drugs. *Proc Natl Acad Sci USA* **104**(29):11927-11932.
- Blumberg B, Sabbagh W, Jr., Juguilon H, Bolado J, Jr., van Meter CM, Ong ES and Evans RM (1998) SXR, a novel steroid and xenobiotic-sensing nuclear receptor. *Genes Dev* **12**(20):3195-3205.
- Bohl CE, Chang C, Mohler ML, Chen J, Miller DD, Swaan PW and Dalton JT (2004) A ligand-based approach to identify quantitative structure-activity relationships for the androgen receptor. *J Med Chem* **47**(15):3765-3776.
- Chan V, Charles BG and Tett SE (2005) Population pharmacokinetics and association between A77 1726 plasma concentrations and disease activity measures following administration of leflunomide to people with rheumatoid arthritis. *Br J Clin Pharmacol* **60**(3):257-264.
- Chang C, Bahadduri PM, Polli JE, Swaan PW and Ekins S (2006a) Rapid Identification of P-glycoprotein Substrates and Inhibitors. *Drug Metab Dispos* **34**:1976-1984.

- Chang C, Ekins S, Bahadduri P and Swaan PW (2006b) Pharmacophore-based discovery of ligands for drug transporters. *Adv Drug Del Rev* **58**:1431-1450.
- Chen Y, Tang Y, Wang MT, Zeng S and Nie D (2007) Human pregnane X receptor and resistance to chemotherapy in prostate cancer. *Cancer Res* **67**(21):10361-10367.
- Chrencik JE, Orans J, Moore LB, Xue Y, Peng L, Collins JL, Wisely GB, Lambert MH, Kliewer SA and Redinbo MR (2005) Structural disorder in the complex of human pregnane X receptor and the macrolide antibiotic rifampicin. *Mol Endocrinol* **19**(5):1125-1134.
- Clement OO and Mehl AT (2000) HipHop: Pharmacophore based on multiple common-feature alignments, in *Pharmacophore perception, development, and use in drug design* (Guner OF ed) pp 69-84, IUL, San Diego.
- Das BC, Madhukumar AV, Kim S, Sinz M, Zvyaga TA, Power EC, Ganellin CR and Mani S (2008) Synthesis of novel ketoconazole derivatives as antagonists of the human Pregnane X Receptor (PXR; NR1I2; also termed SXR, PAR). *Bioorg Med Chem Letts* **In Press**.
- Dilmaghanian S, Gerber JG, Filler SG, Sanchez A and Gal J (2004) Enantioselectivity of inhibition of cytochrome P450 3A4 (CYP3A4) by ketoconazole: Testosterone and methadone as substrates. *Chirality* **16**(2):79-85.
- Ekins S, Chang C, Mani S, Krasowski MD, Reschly EJ, Iyer M, Kholodovych V, Ai N, Welsh WJ, Sinz M, Swaan PW, Patel R and Bachmann K (2007) Human pregnane X receptor antagonists and agonists define molecular requirements for different binding sites. *Mol Pharm* **72**:592-603.
- Ekins S, Johnston JS, Bahadduri P, D'Souza VM, Ray A, Chang C and Swaan PW (2005) In Vitro And Pharmacophore Based Discovery Of Novel hPEPT1 Inhibitors. *Pharm Res* **22**:512-517.
- Estebanez-Perpina E, Arnold LA, Nguyen P, Rodrigues ED, Mar E, Bateman R, Pallai P, Shokat KM, Baxter JD, Guy RK, Webb P and Fletterick RJ (2007) A surface on the androgen receptor that allosterically regulates coactivator binding. *Proc Natl Acad Sci USA* **104**(41):16074-16079.

- Evers A, Hessler G, Matter H and Klabunde T (2005) Virtual screening of biogenic amine-binding G-protein coupled receptors: comparative evaluation of protein- and ligand-based virtual screening protocols. *J Med Chem* **48**(17):5448-5465.
- Evers A and Klabunde T (2005) Structure-based drug discovery using GPCR homology modeling: successful virtual screening for antagonists of the alpha1A adrenergic receptor. *J Med Chem* **48**(4):1088-1097.
- Gomella L and Haist S (2004) *Clinician's pocket drug reference 2004*. McGraw-Hill.
- Gupta D, Venkatesh M, Wang H, Kim S, Sinz M, Goldberg GL, Whitney K, Longley C and Mani S (2008) Expanding the Roles for Pregnane X Receptor (PXR) in Cancer: Proliferation and Drug Resistance in Ovarian Cancer. *Clinical Cancer Res* **in press**.
- Healan-Greenberg C, Waring JF, Kempf DJ, Blomme EA, Tirona RG and Kim RB (2007) HIV protease inhibitor A-792611 is a novel functional inhibitor of human PXR. *Drug Metab Dispos* **36**:500-507.
- Hopkins AL, Groom CR and Alex A (2004) Ligand efficiency: a useful metric for lead selection. *Drug Disc Today* **9**(10):430-431.
- Huang H, Wang H, Sinz M, Zoeckler M, Staudinger J, Redinbo MR, Teotico DG, Locker J, Kalpana GV and Mani S (2007) Inhibition of drug metabolism by blocking the activation of nuclear receptors by ketoconazole. *Oncogene* **26**(2):258-268.
- Hurst CH and Waxman DJ (2004) Environmental phthalate monoesters activate pregnane X receptor-mediated transcription. *Toxicol Appl Pharmacol* **199**(3):266-274.
- Johnson DR, Li C-W, Chen L-Y, Ghosh JC and Chen JD (2006) Regulation and Binding of Pregnane X Receptor by Nuclear Receptor Corepressor Silencing Mediator of Retinoid and Thyroid Hormone Receptors (SMRT). *Mol Pharm* **69**:99-108.
- Jones G, Willett P, Glen RC, Leach AR and Taylor R (1997) Development and validation of a genetic algorithm for flexible docking. *J Mol Biol* **267**(3):727-748.
- Kalgutkar AS, Nguyen HT, Vaz AD, Doan A, Dalvie DK, McLeod DG and Murray JC (2003) In vitro metabolism studies on the isoxazole ring scission in the anti-inflammatory agent leflunomide to its

active alpha-cyanoenol metabolite A771726: mechanistic similarities with the cytochrome P450-catalyzed dehydration of aldoximes. *Drug Metab Dispos* **31**(10):1240-1250.

Kliewer SA, Moore JT, Wade L, Staudinger JL, Watson MA, Jones SA, McKee DD, Oliver BB, Willson TM, Zetterstrom RH, Perlmann T and Lehmann JM (1998) An orphan nuclear receptor activated by pregnanes defines a novel steroid signalling pathway. *Cell* **92**:73-82.

Krasowski MD, Yasuda K, Hagey LR and Schuetz EG (2005) Evolution of the pregnane X receptor: adaptation to cross-species differences in biliary bile salts. *Mol Endocrinol* **19**(7):1720-1739.

Leach AR, Shoichet BK and Peishoff CE (2006) Prediction of protein-ligand interactions. Docking and scoring: successes and gaps. *J Med Chem* **49**(20):5851-5855.

Lemaire G, Benod C, Nahoum V, Pillon A, Boussioux AM, Guichou JF, Subra G, Pascussi JM, Bourguet W, Chavanieux A and Balaguer P (2007) Discovery of a highly active ligand of human Pregnane X Receptor: a case study from pharmacophore modeling and virtual screening to "in vivo" biological activity. *Mol Pharmacol* **72**:572-581.

Mani S, Huang H, Sundarababu S, Liu W, Kalpana G, Smith AB and Horwitz SB (2005) Activation of the steroid and xenobiotic receptor (human pregnane X receptor) by nontaxane microtubule-stabilizing agents. *Clin Cancer Res* **11**(17):6359-6369.

Moore LB, Parks DJ, Jones SA, Bledsoe RK, Consler TG, Stimmel JB, Goodwin B, Liddle C, Blanchard SG, Willson TM, Collins JL and Kliewer SA (2000) Orphan nuclear receptors constitutive androstane receptor and pregnane X receptor share xenobiotic and steroid ligands. *J Biol Chem* **275**(20):15122-15127.

Reynolds CH, Tounge BA and Bembenek SD (2008) Ligand binding efficiency: trends, physical basis, and implications. *J Med Chem* **51**(8):2432-2438.

Rozman B (2002) Clinical pharmacokinetics of leflunomide. *Clinical pharmacokinetics* **41**(6):421-430.

Schapira M, Abagyan R and Totrov M (2003a) Nuclear hormone receptor targeted virtual screening. *J Med Chem* **46**(14):3045-3059.

- Schapira M, Raaka BM, Das S, Fan L, Totrov M, Zhou Z, Wilson SR, Abagyan R and Samuels HH (2003b) Discovery of diverse thyroid hormone receptor antagonists by high-throughput docking. *Proc Natl Acad Sci USA* **100**(12):7354-7359.
- Schapira M, Raaka BM, Samuels HH and Abagyan R (2000) Rational discovery of novel nuclear hormone receptor antagonists. *Proc Natl Acad Sci USA* **97**:1008-1013.
- Schapira M, Raaka BM, Samuels HH and Abagyan R (2001) In silico discovery of novel retinoic acid receptor agonist structures. *BMC Structural Biol* **1**(1).
- Schuetz E and Strom S (2001) Promiscuous regulator of xenobiotic removal. *Nature medicine* **7**:536-537.
- Synold TW, Dussault I and Forman BM (2001) The orphan nuclear receptor SXR coordinately regulates drug metabolism and efflux. *Nature Medicine* **7**:584-590.
- Tabb MM, Kholodovych V, Grun F, Zhou C, Welsh WJ and Blumberg B (2004) Highly chlorinated PCBs inhibit the human xenobiotic response mediated by the steroid and xenobiotic receptor (SXR). *Environ Health Perspect* **112**(2):163-169.
- Ung CY, Li H, Yap CW and Chen YZ (2007) In silico prediction of pregnane X receptor activators by machine learning approaches. *Mol Pharm* **71**(1):158-168.
- Wang CY, Li CW, Chen JD and Welsh WJ (2006) Structural model reveals key interactions in the assembly of the pregnane X receptor/corepressor complex. *Mol Pharm* **69**(5):1513-1517.
- Wang H, Huang H, Li H, Teotico DG, Sinz M, Baker SD, Staudinger J, Kalpana G, Redinbo MR and Mani S (2007) Activated PXR is a target for ketoconazole and its analogs. *Clin Cancer Res* **13**(8):2488-2495.
- Wang H, Li H, Moore LB, Maglich JM, Goodwin B, Ittopp ORR, Wisely B, Creech K, Parks DJ, Collins JL, Willson TM, Kalpana GV, Xie W, Redinbo MR, Moore JT and Mani S (2008) The phytoestrogen coumestrol is a naturally-occurring antagonist of the pregnane X receptor (PXR). *Mol Endocrinol*, **In press**.
- Watkins RE, Davis-Searles PR, Lambert MH and Redinbo MR (2003) Coactivator binding promotes the specific interaction between ligand and the pregnane X receptor. *J Mol Biol* **331**:815-828.

- Xue Y, Chao E, Zuercher WJ, Willson TM, Collins JL and Redinbo MR (2007a) Crystal structure of the PXR-T1317 complex provides a scaffold to examine the potential for receptor antagonism. *Bioorg Med Chem* **15**(5):2156-2166.
- Xue Y, Moore LB, Orans J, Peng L, Bencharit S, Kliewer SA and Redinbo MR (2007b) Crystal structure of the pregnane X receptor-estradiol complex provides insights into endobiotic recognition. *Mol Endocrinol* **21**(5):1028-1038.
- Zhang T, Zhou JH, Shi LW, Zhu RX and Chen MB (2007) 3D-QSAR studies with the aid of molecular docking for a series of non-steroidal FXR agonists. *Bioorg Med Chem Lett* **17**(8):2156-2160.
- Zhou C, Poulton EJ, Grun F, Bammler TK, Blumberg B, Thummel KE and Eaton DL (2007) The dietary isothiocyanate sulforaphane is an antagonist of the human steroid and xenobiotic nuclear receptor. *Mol Pharm* **71**(1):220-229.

FOOTNOTES PAGE

a) Unnumbered footnotes

Equal contribution (SE, SM)

b) S.E., N.A., V. K., and W.J.W. gratefully acknowledge the support for this work provided by the USEPA-funded Environmental Bioinformatics and Computational Toxicology Center (ebCTC), under STAR Grant number GAD R 832721-010. This work was supported in part by a grant from the Damon Runyon Cancer Research Foundation (CI: 15-02 to S.M).

c) Send reprint requests to:

Sean Ekins, D.Sc., Collaborations in Chemistry, 601 Runnymede Avenue, Jenkintown, PA 19046. Email ekinssean@yahoo.com

d)

Collaborations in Chemistry, 601 Runnymede Avenue, Jenkintown, PA 19046 (SE)

Department of Pharmaceutical Sciences, University of Maryland, 20 Penn Street, Baltimore, MD 21201 (SE)

Department of Pharmacology, University of Medicine and Dentistry of New Jersey, Robert Wood Johnson

Medical School, 675 Hoes Lane, Piscataway, NJ 08854, USA. (SE, VK, NA, WJW)

Bristol-Myers Squibb Company, Research Parkway, Wallingford, CT 06492

USA (MS)

University of Colorado Denver, School of Medicine, Division of Clinical Pharmacology, Aurora, CO 80045.

(JG)

University of Colorado Denver , School of Medicine , Biochemistry and Molecular Genetics, Aurora, CO 80045. (LG)

Department of Pharmacology, The University of Toledo College of Pharmacy, Toledo, Ohio 43606 (KB)

Albert Einstein Cancer Center, Albert Einstein College of Medicine, Bronx, NY 10461 (SM)

FIGURE LEGENDS

Figure 1. The Enilconazole shape/feature hypothesis for PXR antagonists and fit of coumestrol analogs, sulfuraphane and biphenyls. A. Enilconazole was mapped to the previously described PXR antagonist pharmacophore and a van der Waals surface was created around it. B. Coumestrol, C. Coumestrol diacetate, D. coumestrol dimethyl ether, E. sulfuraphane and F. polychlorinated biphenyls mapped to the PXR antagonist pharmacophore. Note molecules B-F missed between one to two pharmacophore features and therefore the pharmacophore fit score is not comparable to those for molecules in Table 1. Pharmacophore features blue = hydrophobic, Orange ring aromatic/hydrophobic, Green = hydrogen bond acceptor.

Figure 2. Molecules derived from database searching with the PXR antagonist pharmacophore (Ekins et al., 2007). A. indomethacin, B. rosmarinic acid, C. bestatin, D. SPB03064, E. SPB00574, F. SPB03255. Pharmacophore features blue = hydrophobic, Orange ring aromatic/hydrophobic, Green = hydrogen bond acceptor.

Figure 3. SPB03255 and structural analogs showing PXR antagonist activity.

Figure 4. Docking of PXR antagonists in the AF-2 antagonist site. A. side view of ketoconazole, B. front view of ketoconazole, C. side view of coumestrol, D. front view of coumestrol, E. side view of SPB03255, F. front view of SPB03255, G. side view of SPB06257 and H. front view of SPB06257.

Figure 5. Analysis of the single Q272H mutant in a mammalian system. A. PXR transcription studies in CV-1 cells were performed using the Q272H mutant of PXR cloned into a mammalian plasmid. The wild-type PXR plasmid was activated by rifampicin (2.3-fold) and was significantly inhibited by ketoconazole ($p < 0.0001$). The Q272H mutant of PXR was constitutively active and rifampicin did not significantly augment basal activity. However, this mutant was not inhibited by ketoconazole ($p=0.181$). In contrast, the modified

ketoconazole analog (compound 3) inhibited the Q272H mutant in the absence or presence of rifampicin ($p < 0.001$; $p < 0.003$). B. Structure of ketoconazole, C. Structure of 'compound 3' (1-(4-(4-(((2R,4S)-2-(2,4-difluorophenyl)-2-methyl-1,3-dioxolan-4-yl)methoxy)phenyl)piperazin-1-yl)ethanone.

Table 1. Predicted fit of molecules to the PXR antagonist pharmacophore with shape restriction based on itraconazole, GOLD docking scores and biological data for PXR in agonist and antagonist modes.

| Molecule | Database Source | Catalyst | GOLD | Agonist mode | Antagonist mode |
|----------------------------|--|--|----------------------|--|---|
| | | Fit value with shape restriction | Score (AF-2 site) | PXR +DMSO EC ₅₀ ± SEM [§] (μM) | PXR +Rifampicin IC ₅₀ ± SEM [§] (μM) |
| Itraconazole | Similarity to fluconazole using ChemFinder | - | 51.44 | >50* | 8.96 ± 2.6 |
| Indomethacin | SCUT and BIOMOL known bioactives | 1.24 | 35.44 | >50 | >50 |
| Warfarin | SCUT | 1.32 | 41.15 | >50 | >50 |
| Rosmarinic acid | BIOMOL natural products | 1.60 | 35.64 | >50 | >50 |
| Bestatin | BIOMOL known bioactives | 0.61 | 38.30 | >50 | >50 |
| SPB03064 | MiniMaybridge | 2.82 | 42.74 | >50 | >50 |
| SPB00574 | MiniMaybridge | 2.14 | 43.47 | >50 | 24.8 ± 3.2 |
| SPB03255 | MiniMaybridge | 2.22 | 38.22 | >50 | 6.3 ± 1.2 |
| Rifampicin | | | 9.15 | 0.78 ± 0.1 | >50 |
| (+) 2R, 4S Ketoconazole | | | 51.52 | >50 | 16.4 ± 0.3 |
| (-) 2S, 4R Ketoconazole | | | 51.80 | >50 | 16.6 ± 0.3 |

| | | | | MOL #49437 |
|-----------------|---------------------|-------|-----|-------------------|
| S- Sulforaphane | (2.30) ⁺ | 30.47 | >50 | 5.64 ± 3.1 |
| R- Sulforaphane | (1.90) ⁺ | 30.42 | >50 | 5.58 ± 3.6 |
| Coumestrol | 1.30 | 33.35 | >50 | 12 ⁺⁺ |

[§] Standard error of mean (SEM) calculated from 3 sets of experiments each in duplicate; those >50 were all >50 so SEM = 0.

* >50 = inactive

⁺ = only maps 2 of 4 pharmacophore features using 'ligand pharmacophore mapping mode' allowing rigid mapping and 2 features missed

⁺⁺ value previously published as an antagonist of SR12813, also antagonizes rifampicin mediated induction in human hepatocytes (Wang et al., 2008)

Molecule structures for indomethacin, rosmarinic acid, bestatin, SPB03064, SPB00574 and SPB03255 are shown in Figure 2.

Table 2. Predicted and observed results using the PXR antagonist pharmacophores, GOLD docking scores and biological data after using the antagonist lead SPB03255 for substructure searching with ChemSpider and eMolecules.

| Molecule | Catalyst | Catalyst | Catalyst | GOLD | Agonist mode | Antagonist |
|------------------|----------------------|------------------------|------------------|-------------------------|---|--|
| | shape fit - rigid | shape fit- flexible | hypo fit only | Score (AF-2 site) | PXR +DMSO EC ₅₀ [#] (μM) | mode PXR +RIF IC ₅₀ [#] (μM) |
| SPB03256 | 0.71 | 1.62 | 2.11 | 40.80 | >50 | 6.21 |
| SPB03254 | 1.76 | 1.49 | 1.76 | 43.24 | 5.23 | >50 |
| SPB06061 | - | - | 0.62 | 37.54 | >50 | 5.22 |
| SPB03259 | - | - | 0.59 | 36.80 | >50 | >50 |
| SPB03211 | 0.7 | 1.43 | 1.81 | 36.76 | 13.59 | >50 |
| SPB03213 | - | - | 1.7 | 36.65 | 1.71 | >50 |
| SPB03214 | 1.68 | 2.89 | 1.76 | 36.22 | >50 | >50 |
| SPB03215 | - | 1.37 | 1.62 | 33.64 | >50 | >50 |
| SPB03650 | 1.62 | 3.01 | 1.93 | 40.84 | NT | NT |
| SPB03651 | - | - | - | 35.81 | >50 | >50 |
| SPB03212 | - | - | - | 33.09 | NT | NT |
| SPB03663 | - | - | - | 37.55 | 16.83 | >50 |
| pubchem- 3169346 | - | 2.26 | 0.72 | 39.81 | NT | NT |
| SPB06257 | - | 2.66 | 2.05 | 47.26 | >50 | 16.42 |
| SPB02372 | - | - | 1.44 | 42.16 | >50 | 5.82 |
| SPB06166 | - | - | - | 38.52 | NT | NT |
| SPB06259 | 1.1 | 2.72 | 1.95 | 44.88 | NT | NT |
| Leflunomide | - | - | - | 31.00 | >50 | 6.80 |

Data represents single runs in duplicate.

Docking scores in bold were the highest in the molecules tested *in vitro*.

NT = not tested

- = no fit

All molecule structures are shown in Figure 3 and Supplemental Figure 2.

Table 3 Calculated physicochemical properties and ligand efficiency indices.

| Molecule | pIC ₅₀ | PSA ⁺ (Å ²) | ALogP ⁺ | Molecular_Weight ⁺ | | | | |
|--------------|-------------------|------------------------------------|--------------------|-------------------------------|-----------------|------------------|-------|-------|
| | | | | (Da) | HA [#] | LE ^{\$} | BEI* | SEI* |
| SPB06257 | 4.78 | 50.05 | 4.69 | 339.41 | 24 | 0.20 | 14.10 | 9.56 |
| SPB02372 | 5.24 | 41.12 | 6.36 | 398.69 | 24 | 0.22 | 13.13 | 12.73 |
| Leflunomide | 5.17 | 53.93 | 2.16 | 270.21 | 19 | 0.27 | 19.12 | 9.58 |
| Coumestrol | 4.92 | 76.79 | 1.39 | 270.24 | 20 | 0.25 | 18.21 | 6.41 |
| Itraconazole | 5.05 | 96.69 | 6.43 | 705.63 | 49 | 0.10 | 7.15 | 5.22 |
| SPB00574 | 4.61 | 48.69 | 5.94 | 386.68 | 23 | 0.20 | 11.91 | 9.46 |
| Ketoconazole | 4.78 | 67.41 | 3.61 | 531.43 | 36 | 0.13 | 9.00 | 7.10 |
| Sulforaphane | 5.25 | 28.62 | 1.16 | 177.29 | 10 | 0.52 | 29.61 | 18.34 |
| SPB03255 | 5.20 | 64.93 | 3.88 | 314.36 | 22 | 0.24 | 16.54 | 8.01 |
| SPB03256 | 5.21 | 64.93 | 4.34 | 368.33 | 25 | 0.21 | 14.14 | 8.02 |
| SPB06061 | 5.28 | 64.93 | 3.39 | 300.33 | 21 | 0.25 | 17.59 | 8.14 |

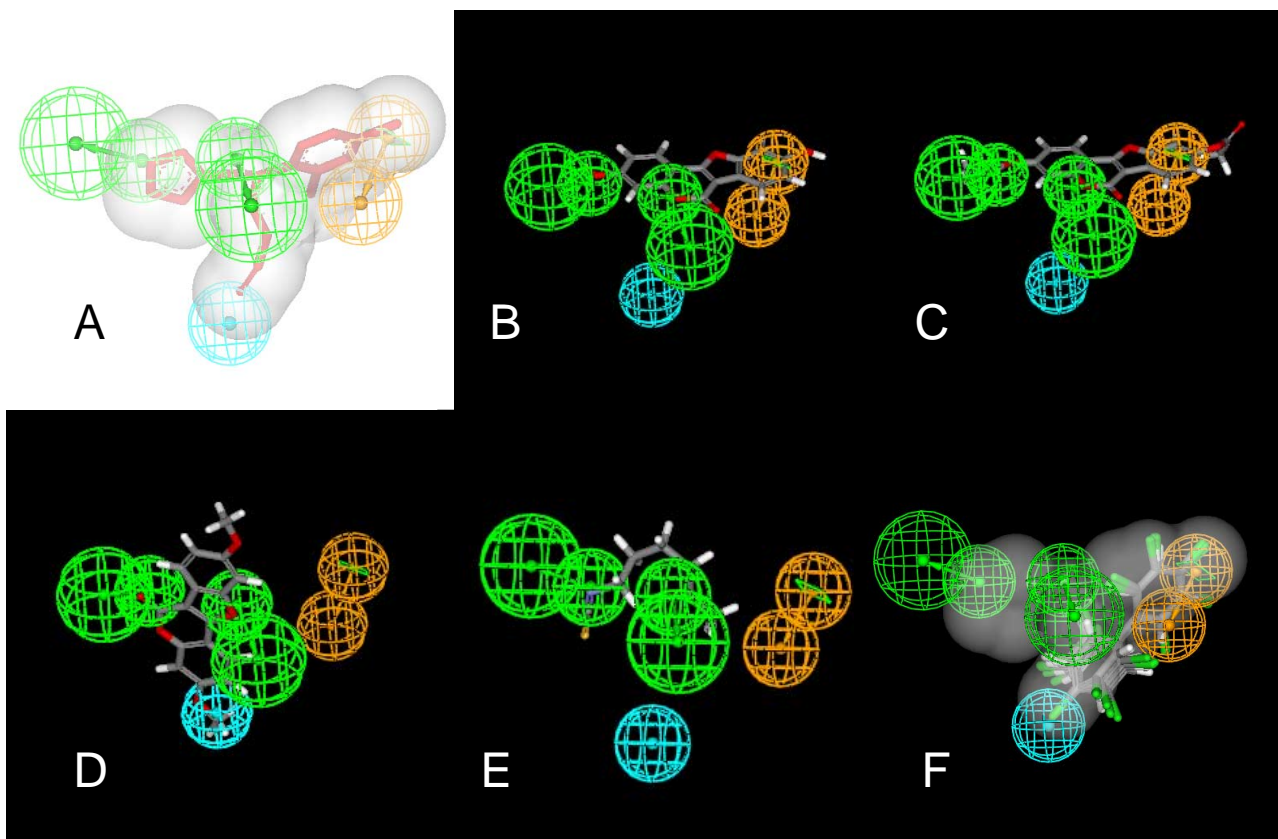
⁺ PSA, Polar surface area, and other properties calculated using Accelrys Discovery Studio 2.0.

[#] HA, heavy atom count.

^{\$} LE, Ligand efficiency = pIC₅₀/HA (Reynolds et al., 2008).

*BEI, Binding efficiency Index = pIC₅₀/molecular weight (kDa); SEI, Surface-binding efficiency index = pIC₅₀/PSA (Abad-Zapatero and Metz, 2005).

Fig 1



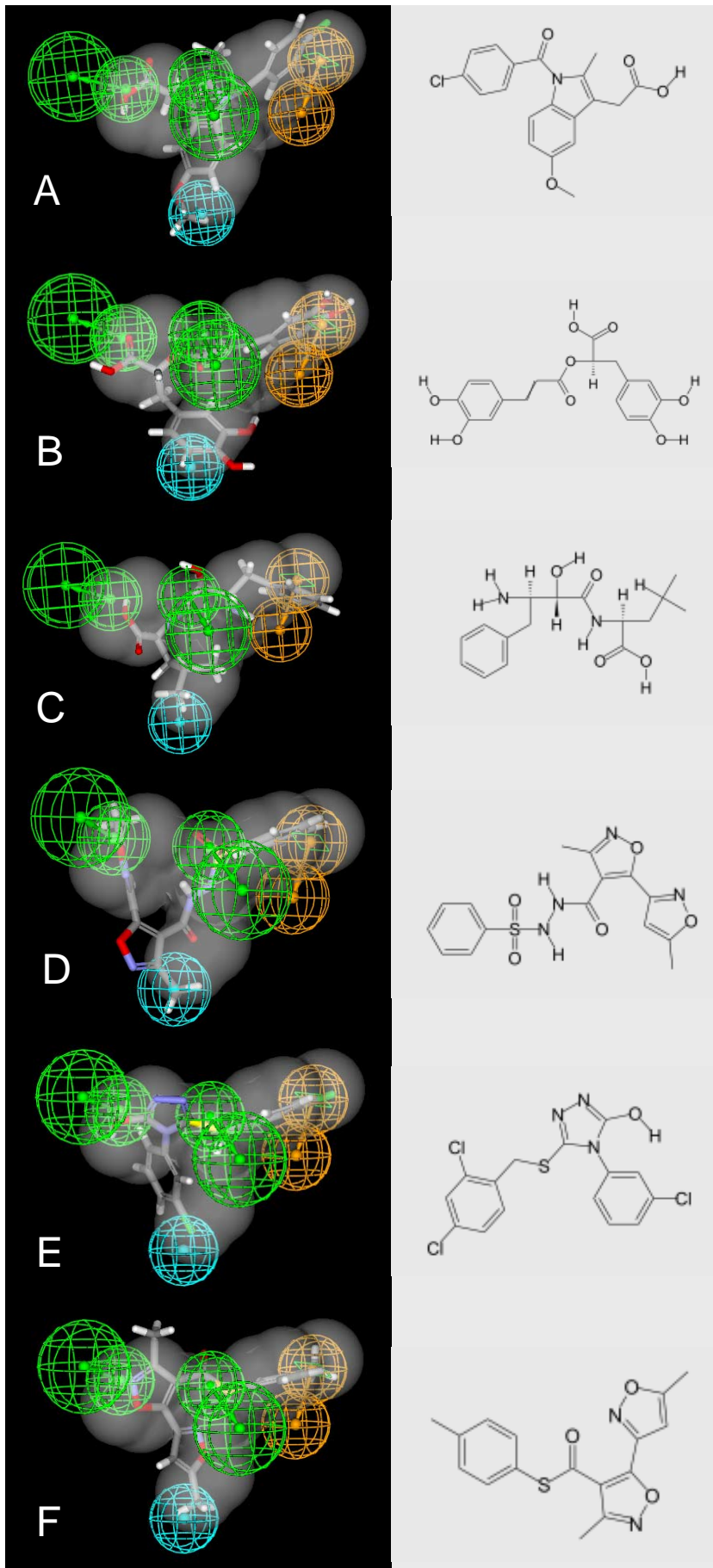


Fig 2

Fig 3

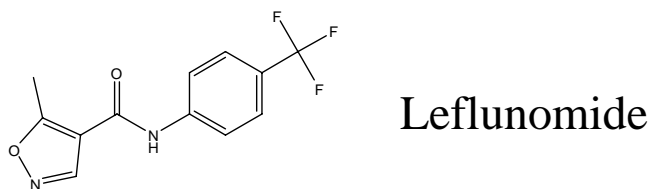
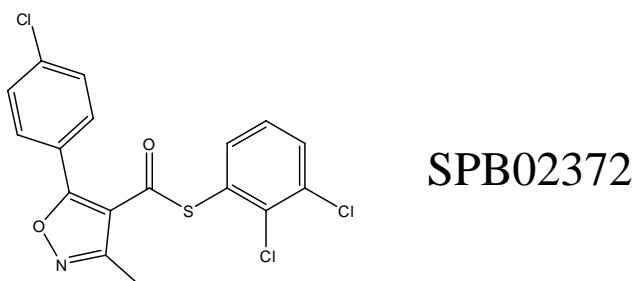
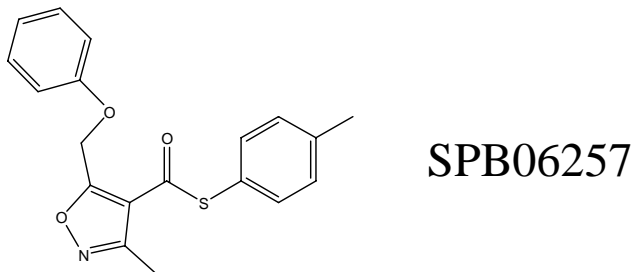
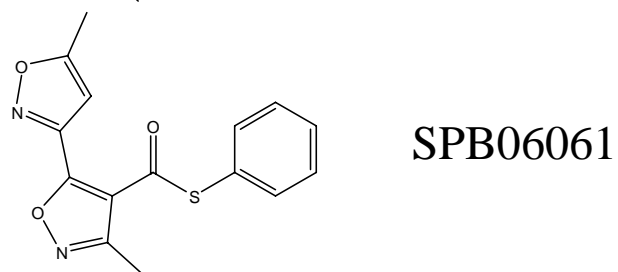
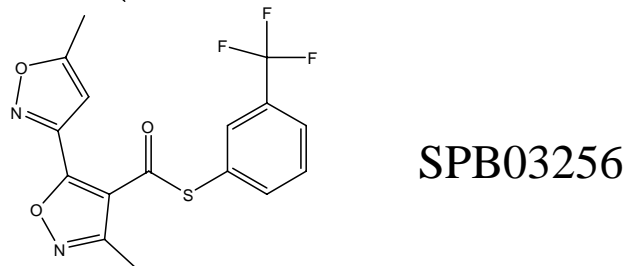
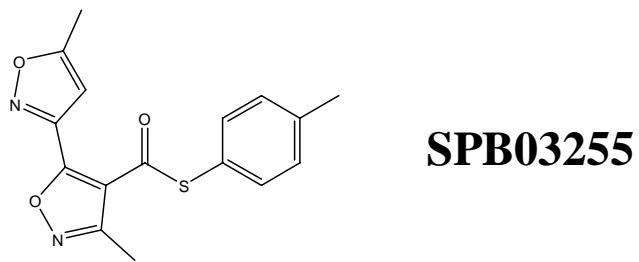


Fig 4

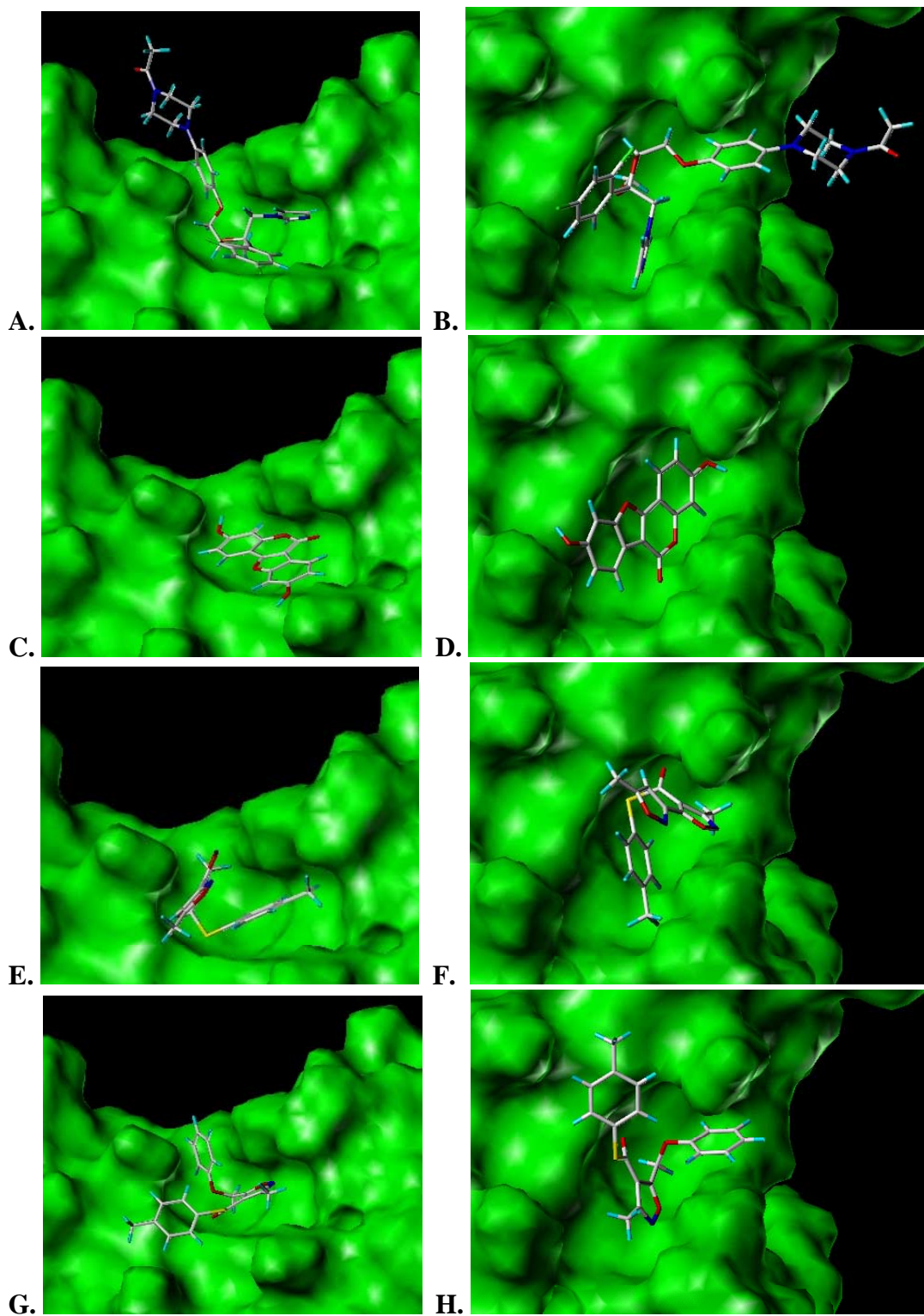


Fig 5

